*Polish Journal of Chemical Technology, 17, **4**, 74 — 81, 10.1515/pjct-2015-0071*

Thermoplastic elastomers containing 2D nanofillers: montmorillonite, graphene nanoplatelets and oxidized graphene platelets

Sandra Paszkiewicz[1*], Iwona Pawelec[2], Anna Szymczyk[2], Zbigniew Rosłaniec[1]

[1]*West Pomeranian University of Technology, Szczecin, Institute of Material Science and Engineering, Piastow Av. 19, 70-310 Szczecin, Poland*
[2]*West Pomeranian University of Technology, Szczecin, Institute of Physics, Piastow Av. 19, 70-310 Szczecin, Poland*
[*]*Corresponding author: e-mail: spaszkiewicz@zut.edu.pl*

This paper presents a comparative study on which type of platelets nanofiller, organic or inorganic, will affect the properties of thermoplastic elastomer matrix in the stronger manner. Therefore, poly(trimethylene terephthalate-block-poly(tetramethylene oxide) copolymer (PTT-PTMO) based nanocomposites with 0.5 wt.% of clay (MMT), graphene nanoplatelets (GNP) and graphene oxide (GO) have been prepared by *in situ* polymerization. The structure of the nanocomposites was characterized by transmission electron microscopy (TEM) in order to present good dispersion without large aggregates. It was indicated that PTT-PTMO/GNP composite shows the highest crystallization temperature. Unlike the addition of GNP and GO, the introduction of MMT does not have great effect on the glass transition temperature of PTMO-rich soft phase. An addition of all three types of nanoplatelets in the nanocomposites caused the enhancement in tensile modulus and yield stress. Additionally, the cyclic tensile tests showed that prepared nanocomposites have values of permanent set slightly higher than neat PTT-PTMO.

Keywords: montmorillonite, graphene oxide, graphene nanoplatelets, thermoplastic elastomers, *in situ* polymerization.

INTRODUCTION

Recently, research and development of polymer nanocomposites, started to get an interesting topic in the field of materials science and engineering. These materials possess a number of interesting properties, among others: high modulus values, high impact strength, low density, which provides a weight's savings, barrier properties with respect to gases' penetration, electrical conductivity etc. These advantages occur at low content of nanofillers in the composite (less than 10%), but usually it is about 3–5% by weight. Such low content of nanoparticles did not significantly affect the processing properties of these materials, but significantly facilitates their recycling. As nanofillers can be used materials being different in the terms of chemical nature (organic and inorganic), physical structure (among others: crystalline, amorphous, gas inclusions), as well as the shape of particles (3D-powder, 2D-platelets and 1D-linear, fibers, tubes).

Among many types of polymers nanocomposites, which so far have appeared and are widely used in the industrial applications, polymer–clay nanocomposites attracted most of the attention, since firstly reported by the Toyota research group on a nylon-6/montmorillonite material[1, 2]. Montmorillonite (MMT), with the layer thickness of around 1 nm and the lateral dimensions of layers varied from 30 nm to several microns or more (depending on the particular silicate's type) is the most widely used clay, which naturally occurs. Moreover it has the same layered and crystal line structure as talc and mica but a different layer charge[3]. So far, the numerous studies have confirmed the effectiveness of adding MMT to nanocomposites, among others to epoxy[4], unsaturated polyester[5], polyamide[6], polystyrene[7], polypropylene[8] and poly(ethylene terephthalate)[9] etc. In each case, the incorporation of layered silicates resulted in obtaining materials that exhibited high stiffness, strength and gas barrier properties at a much smaller content than it was used in conventional polymer composites (containing micron-sized fillers). However, the discovery in 2004 of the new carbon allotrope, namely graphene, due to its extraordinary physico-chemical properties attracted much attention on nanocomposites with its participation. Graphene is an atomically thick, two-dimensional (2-D) sheet composed of sp2 carbon atoms arranged in a honeycomb structure[10] with a carbon–carbon bond length of 0.142 nm[11], extremely high surface area and gas impermeability[12], very high electrical conductivity[13], exceptional thermal conductivity[14] and superior mechanical properties (Young's modulus of 1 TPa and ultimate strength of 130GPa)[15]. Due to these exceptional properties graphene and graphene derivatives demonstrated great potential for improving electrical, mechanical, thermal, and gas barrier properties of polymers, including poly(vinyl fluoride) (PVF)[16], poly(ethylene) (PE)[17], polystyrene (PS)[18], PMMA[19], Nylon 6[20], polyurethanes (PU)[21], poly (butylene terephthalate) (PBT)[22], poly(ethylene terephthalate) (PET)[23–25] etc. However, one should consider that the properties of polymer nanocomposites depend significantly on the degree of nanoparticles' dispersion and their uniform distribution throughout the whole volume of the polymer matrix. These conditions are usually quite difficult to carry out, because due to their small size, nanoparticles tend to form aggregates (agglomerates) and tend to increase the total viscosity of the polymer composition. Chemical functionalization of graphene's surface by either oxidation procedure or physical adsorption/grafting protocols have been found to be a feasible and effective method in improving the dispersion of nanoplatelets in organic and/or aqueous media[26]. Additionally, the attached functional groups may enhance the interfacial interactions between the graphenes and the polymer matrix. Polymer nanocomposites with graphene oxide have shown dramatic improvements in properties such as elastic modulus, tensile strength and thermal stability at very low nanofillers' loading[27–29].

In our previous works[29–30], the conditions for the synthesis of nanocomposites with a high degree of MMT and

GO nanoplatelets' exfoliation in PTT-PTMO copolymer matrix have been established. In this work the effect of three different types of 2D nanofillers i.e. MMT, GNP and GO on structure and mechanical properties of nanocomposites based on poly(trimethylene terephthalate-*-block*-tetramethylene oxide) (PTT-PTMO) copolymer was studied. To the best of our knowledge, there is no report on comparing the influence of MMT, GNP and GO at the same nanoplatelets content (0.5 wt.%) on the PTT-PTMO copolymer matrix.

EXPERIMENTAL

Nanofillers

As 2D nanofillers the following materials were used:

– as a high purity layered silicate based on montmorillonite, the organoclay Nanofil 32 (Süd-Chemie, Germany) modified by stearylbenzyldimethyl ammonium chloride, a weight loss of 35.3 wt.% in the temperature range of 200–650°C and with an average particle size of about 30 μm has been used. The detailed characterization of the nanofiller has been already published in[30].

– graphene nanoplatelets (GNP) were purchased form ANGSTRON Materials (Dayton, Ohio, USA) in the form of a powder with the thickness of less than three graphene layers, average platelets size of up to 10 μm, carbon content of ~97.0% and the oxygen content of ~2.10%.

– graphene oxide (GO) with an average particle size of 50 μm was provided from Polymer Institute of Slovak Academy of Science and prepared by Brodie oxidation method already reported in[31]. The detailed characterization of GO (SEM, XPS) will be found in our previous publication[29].

In situ synthesis of PTT-PTMO based nanocomposites

Nanocomposites based on PTT-PTMO copolymer with three types of 2D nanofillers (MMT, GNP and GO) were synthesised by melt transesterification and subsequently polycondensation following the procedure described previously in[29, 30, 32, 33]. In the first stage, an appropriate amount of nanoplatelets was dispersed in 1,3-propanediol (PDO, Shell Chemicals) using ultra-high speed (Ultra-Turax T25) and sonicator (Homogenizer HD 2200, Sonoplus, with a frequency of 20 kHz and 75% of power 200 W) in each case for 30 min. Additionally, to improve the dispersion/exfoliation of GNP and GO in PDO, an ultra-power lower sonic bath (BANDELIN, Sonorex digitec, with frequency of 35 kHz and power 140 W) was applied for 8 hours. Then the prepared dispersion of nanoplatelets in PDO, along with dimethyl terephthalate (DMT, Sigma-Aldrich) and tetrabutyl orthotitaniate (TBT, Fluka) catalyst was charged into 1 dm^3 steel reactor (Autoclave Engineers Inc, USA). In the first step, the transesterification reaction was carried out under a low nitrogen flow at 165°C for 1.5 hour in the presence of TBT catalyst. When the first step was completed, the poly(tetramethylene oxide) glycol with a molecular weight of 1000 g/mol (PTMG, Terathane 1000, DuPont, USA), Irganox 1010 (Ciba-Geigy, Switzerland, used as thermal stabilizer) and second portion of catalyst (TBT) were added. In the second step, the polycondensation reaction was allowed to proceed at a temperature of 250°C under reduced pressure of ~15 Pa. Synthesis was finished when the melt reached a melt viscosity's value corresponding to the high molecular weight copolymer. The obtained nanocomposite was extruded from the reactor under nitrogen flow, cooled to room temperature in the water bath and then granulated. The neat PTT-PTMO copolymer (without nanoplatelets' content) was synthesized following the same procedure.

Methods of characterization

Transmission electron microscopy (TEM) analysis was carried out by a JEOL JEM-1200 Electron Microscope. The TEM samples were obtained by cutting a piece (thickness of about 70 nm) from the middle part of the tensile specimen's under cryogenic conditions using a Leica EM FCS ultramicrotome.

The average molecular weight of copolymers was determined by using size exclusion chromatography (SEC) on a Waters GPC instrument, equipped with a Shimadzu LC-10AD pump, a WATERS 2414 differential refraction index detector (at 35°C) and a MIDAS auto-injector (50 mL injection volume) following the same procedure as described previously in[34].

The density was measured at 2°C on hydrostatic balance (Radwag WPE 600C, Poland), calibrated for standards with known density.

The thermal behaviour of samples was studied using differential scanning calorimetry (DSC, TA Instrument Q-100). Samples of 10 mg weight were encapsulated into the aluminium pan and then heated from –100 to 250°C at a scan rate of 10°C/min. Subsequently, the samples were cooled to –100°C and then heated again to 250°C using the same scan rate. The second heating and cooling scans were used to determine the melting and crystallization peaks. The glass transition temperature (T_g) for the samples was taken as the midpoint of the heat capacity's change (ΔCp/2). The degree of crystallinity (x_c) was calculated using the following equation:

$$x_c = (\Delta H_m / \Delta H_m^o)$$

where ΔH_m is derived from melting peak area on DSC thermograms and is the enthalpy change of melting for a 100% crystalline standard. The enthalpy value of 145.6 J/g[35] was used for a 100% crystalline PTT. Moreover, the value of supercooling ($\Delta T = T_m - T_c$), which is used to measure the rate of crystallisation, was calculated.

Tensile measurements were performed on the universal testing machine (Instron 5566), equipped with a 5 kN Instron load cell, an contact optical long travel extensometer and the Bluehill 2 software. The measurements were carried out at room temperature using a cross-head speed of 100 mm/min and a grip distance of 20 mm. The tensile properties were determined on injection moulded dumbbell-shaped samples (ISO 37 type 3). The following parameters were determined: Young's modulus, yield stress and strain, stress and elongation at break of the nanocomposites. Six measurements were conducted for each sample, and the results were averaged to obtain a mean value. Moreover, the tensile deformation recovery properties of the samples were investigated (200 mm/min at room temperature, and then the imposed strength was unloaded). Four predetermined strains 20, 50, 100 and 200% were used in our testing.

RESULTS AND DISCUSSION

Dispersion of 2D nanofillers in the polymer matrix

PTT-PTMO based nanocomposites with three different types of 2D nanofillers, synthesized via *in situ* polymerization, exhibited a high-quality dispersion of nanoplatelets throughout the polymer matrix, as determined by TEM micrographs shown in Figure 1. Previous observations on PTT-PTMO/MMT nanocomposites[30] have shown that different degrees of intercalation were present beside the exfoliated layers. However, at lower magnification (Fig. 1a) randomly distributed silicate layers were herein observed. In the case of PTT-PTMO/0.5GNP (Fig. 1b) nanocomposite, the bent or crumpled/wrinkled platelets were visible. Exfoliated graphene-based materials are often compliant and when dispersed in a polymer matrix are typically not observed as rigid disks (flat platelets), but rather as wrinkled ones. Moreover, randomly oriented, exfoliated platelets were observed, possibly due to restacking of the platelets. The processing technique, by means of *in situ* polymerization, could induce orientation of the dispersed platelets, which can be beneficial for reinforcement but may raise the percolation threshold[36]. Finally, the dispersion state and distribution of GO in PTT-PTMO matrix were characterized by TEM (Fig. 1c). Good distribution of GO in PTT-PTMO matrix, shows the presence of GO platelets with "folded" morphology. This may be due to a number of oxygen-containing functional groups on the GO surface and electrostatic repulsion between the negative charges of GO sheets. One can conclude, that both carbon nanofillers: GNP and GO would have been very well dispersed in PDO at the level of individual sheets (by mechanical and ultrasonic treatment), clearly exhibiting a flake-like shape, indicating that that in situ polymerization is a highly efficient method for preparing nanocomposites with 2D-type nanofillers.

Physical properties

As the polymer matrix, the thermoplastic segmented block copolymer, containing 50 wt.% of poly(trimethylene terephthalate), as the rigid segment and 50 wt.% of PTMO as the flexible one, has been applied. Nanocomposites with three types of 2D nanofillers i.e. MMT, GNP and GO, as the same nanofillers' content (0.5 wt.%) have been studied. The composition and physical properties of the obtained nanocomposites are presented in Table 1. All three nanocomposites exhibited high molecular weights. Values of number average molecular weights for nanocomposites with MMT and GNP are varied between 56 450 and 57 400 g/mol (Table 1) and they are close to the value obtained for the neat PTT-PTMO block copolymer (56 700 g/mol). Only GO provided a slight decrease in Mn, along with an increase in polydispersity, which may result from the strong interactions between functional groups on the surface of GO and PTT-PTMO that caused an increase in the viscosity of the melt, as well as from the size of GO platelets (~50 μm), if compared to MMT (~30 μm) and GNP (~10 μm).

Moreover, all three types of nanocomposites, in comparison to the neat copolymer, exhibited comparable values of density. However, slightly higher values of d,

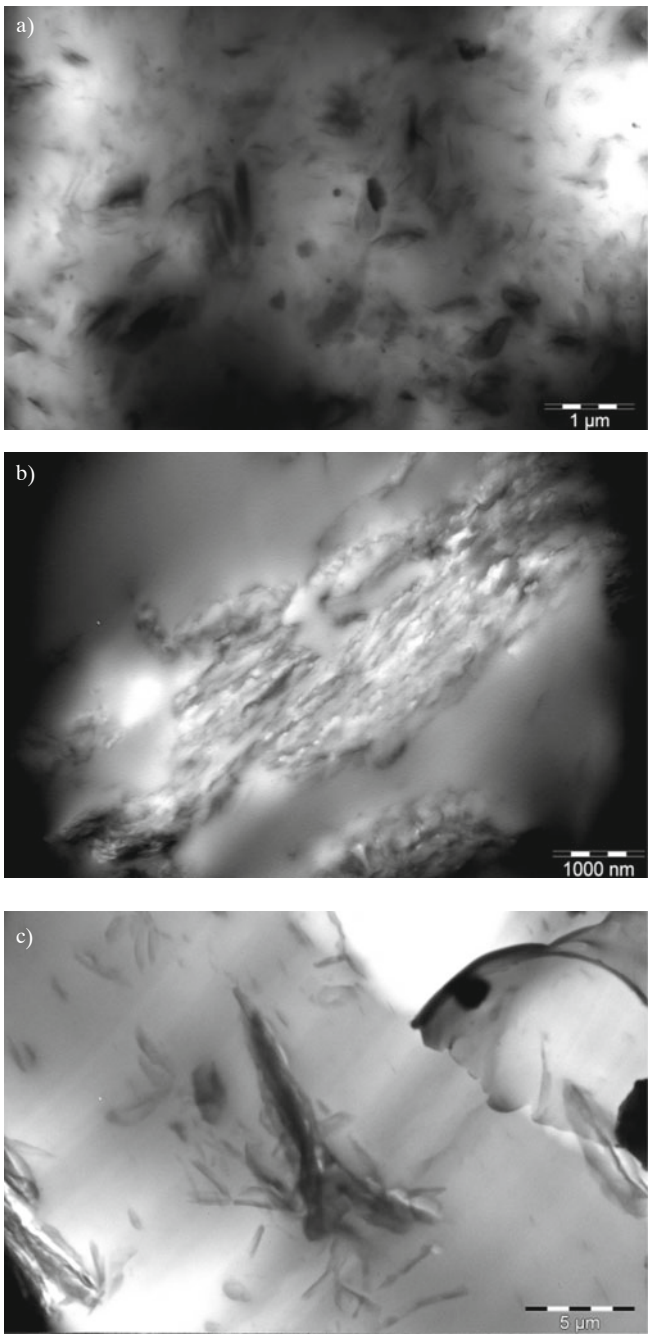

Figure 1. TEM micrographs of: a) PTT-PTMO/0.5MMT; b) PTT-PTMO/0.5GNP and c) PTT-PTMO/0.5GO

obtained for the samples with GNP and GO, might be due to better compatibility of carbon nanoparticles with the polymer matrix through a large number of defects, free radicals and other irregularities on the surface of nanoplatelets (in the case of GNP) or through chemical bonding between hydroxyl and carboxyl groups on the surface of GO[37].

Thermal properties (DSC)

Multiblock copoly(ether-esters) belong to the group of thermoplastic elastomers, which can be characterized by functional properties, similar to vulcanized rubber and a typical method for processing. These types of copolymers have the ability to micro and nano phase separation and reproducible processing conditions. Their specific characteristics result from the domain structure in a condensed state, which consists of two phases: soft and hard. The soft amorphous phase is a homogenous

Table 1. Composition and physical properties of prepared nanocomposites

Sample	M_n	M_w/M_n	d
	g/mol		g/cm^3
PTT-PTMO	56 773	1.80	1.172
PTT-PTMO/0.5MMT	56 450	1.78	1.164
PTT-PTMO/0.5GNP	57 543	1.76	1.176
PTT-PTMO/0.5GO	46 900	2.06	1.177

M_n – number-average molecular weight determined by SEC, M_w/M_n – polydispersity, where: M_w is weight-average molecular weight,; d – density.

mixture of PTMO-T flexible and PTT rigid segments, that have not crystallized. The soft phase has a glass transition temperature below room temperature and gives the material its flexibility. The hard phase, in turn, is formed by the crystallized rigid segments and has a high melting temperature. These hard domains are responsible for good mechanical properties. The two-phase structure of this material is characterized by the presence of two characteristic temperatures: T_{g1} – corresponding to the glass transition temperature of amorphous PTMO-rich phase, and T_m – corresponding to the melting of the PTT crystalline phase. The influence of MMT, GNP and GO on the phase separated structure was examined by DSC (Table 2, Fig. 2). DSC analysis showed that the glass transition temperature corresponding to the PTMO-rich amorphous phase (T_{g1}) was clearly affected by the presence of all three types of 2D nanoparticles, but more pronounced in the case of carbon nanofillers. This, almost five degree shift toward lower temperatures, observed for PTT-PTMO/0.5GNP and PTT-PTMO/0.5GO, is probably caused by the change of PTT-PTMO chains' mobility due to the presence of nanofillers. Moreover, the glass transition temperature corresponding to the amorphous rigid segments (T_{g2}) phase was also affected following the same manner as in the case of T_{g1}. However, in this case, the strongest impact on the glass transition temperature exhibited PTT-PTMO/0.5MMT (five degree shift toward lower temperatures). The observed, herein, shifts in the range of glass transition resulted from the influence of the addition of nanoplatelets on the phase separation of PTT-PTMO matrix. As reported by Lewis[38], either an increase or decrease in T_g can be induced depending on the specific interactions. A higher glass transition temperature in epoxy nanocomposites caused by the addition of graphene sheet was also observed by Martin-Gallego et al.[39], who fabricated and tested UV cured nanocomposites. Moreover, Lee et al.[40] showed that the glass transition temperature of graphene nanocomposites was raised, and the corresponding coefficient of thermal expansion was reduced. Besided, Torre et al.[41] showed the strong influence of the preparation route on the thermal properties of polystyrene (PS) nanocomposites. An appreciable reduction in the Tg was observed only for composites obtained from solution, whereas the composites obtained by melt intercalation showed Tg values approximately equal to that of neat polymer. At the same time, Ilčíková et al.[42] investigated the influence of various surface modification of multiwalled carbon nanotubes (MWCNT) on preferential interactions with individual phases of the linear triblock copolymer polystyrene-*b*-polyisoprene-*b*-polystyrene (SIS). It was observed that the activation energy of glass transition of the polystyrene phase in the MWCNT with short polystyrene chains/SIS composite increased significantly when compared with the neat SIS matrix, while the incorporation of MWCNT with cholesteryl groups resulted in the selective increase of activation energy of glass transition of the polyisoprene phase. Therefore, one can conclude, that 2D types nanofillers (MMT, GO, GNP) used in this study showed interactions with semicrystalline polyester phase resulting in disturbing the physical cross-linking, expressed mainly by decrease of T_{g2}. Moreover, in the case of PTT-PTMO based nanocomposites no appreciable difference in the values of heat capacity of soft segments (Δc_{p1}) was detected. It probably stems from the too small amount of organic and inorganic nanoplatelets. Additionally, the melting thermograms (Fig. 2b) of prepared samples showed no major impact of nanofillers' content on the melting temperature T_m, and the occurring differences of $1 \div 2^oC$ are within the margin of the measurement error. However, there are significant differences in the values (size) of thermal effects associated with melting of the crystal phase of nanocomposites compared to the melt of neat PTT-PTMO. This is reflected in the values of the melting enthalpy ΔH_m (Table 2), which in the case of MMT and GO slight increase, whereas in the case of graphene nanoplatelets is slightly reduced. The direct cause of this phenomenon is the change in the quantity of crystalline phase in nanocomposites, as evidenced by the calculated values of degrees of crystallinity. Furthermore, the presence of MMT, GNP and GO in the polymer, affected the shift's effects associated with crystallization. This shift towards higher temperatures of 25–27°C, for MMT and GNP respectively, is significant and relevant to the processing of these materials. In contrast, the addition of GO resulted in no change of T_c. On the basis of crystallization thermograms (Fig. 2a) one can assume about the antinucleating nature of oxidized graphene nanoplatelets as well as about the distinctive nucleating nature of MMT and GNP. However, it does not coincide

Table 2. Thermal properties of PTT-PTMO based nanocomposites

Sample	T_{g1}	Δc_{p1}	T_{g2}	T_m	ΔH_m	T_c	ΔT	ΔH_c	x_c
	°C	J/g	J/g	°C	J/g	°C	°C	J/g	%
PTT-PTMO	–62	0.25	53	204	30.3	123	81	30.3	20.7
PTT-PTMO/0.5MMT	–62	0.23	48	204	32.0	150	54	31.9	21.9
PTT-PTMO/0.5GNP	–67	0.24	49	203	29.9	148	54	29.3	20.5
PTT-PTMO/0.5GO	–67	0.24	51	204	31.5	123	81	32.0	21.6

T_{g1} – glass transition temperature of soft phase; Δc_{p1} – heat capacity of soft segments; T_{g2} – glass transition temperature of semicrystalline polyester phase; T_m – melting temperature of polyester crystalline phase; T_c – crystallizing temperature of polyester crystalline phase; $\Delta T = T_m - T_c$; ΔH_m, ΔH_c – enthalpy of melting and crystallization of polyester crystals, respectively, x_c – mass fraction of crystallinity.

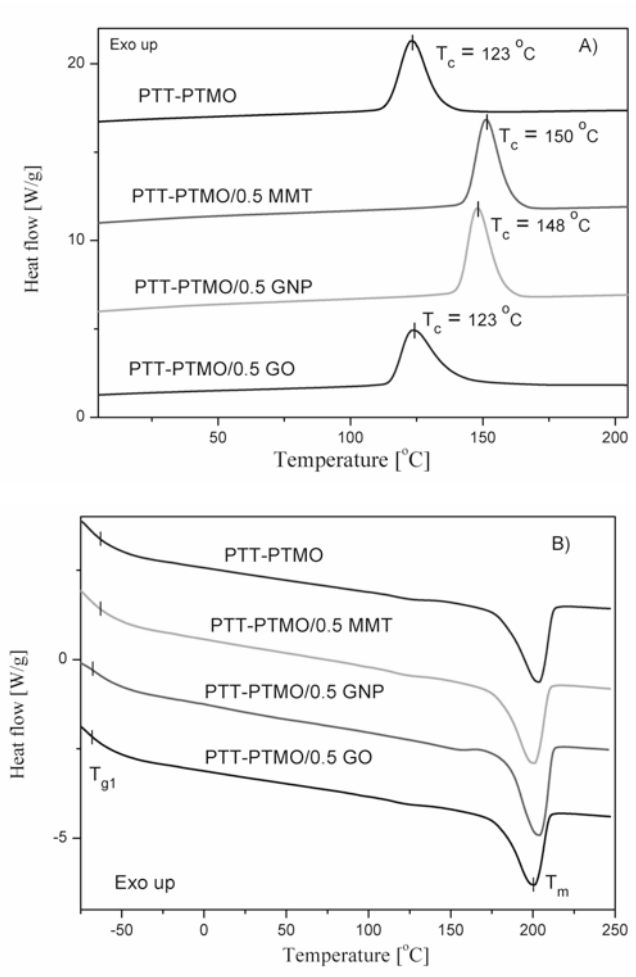

Figure 2. DSC thermograms obtained during cooling (A) and second heating (B) for PTT-PTMO nanocomposites

with the results of the melting enthalpy and the value of the calculated degree of crystallinity, which suggest that in the case of PTT-PTMO/0.5GO no change of crystallization rate could be rather caused by the decrease of the molecular weight of the copolymer (Table 1) than nucleating effect of the additives. Similarly as in the case of PTT-PTMO/0.5MMT and PTT-PTMO/0.5GNP, an increase of the number average molecular weight might result in the increase in crystallization rate.

Mechanical properties of prepared nanocomposites

The reinforcing potential of 2D type plate nanofillers, could be activated when an effective load transfer from the surrounding thermoplastic elastomer matrix into the nanoplatelets and reverse is possible. Therefore, strong interfacial interactions along with good impregnation with the matrix need to be ensured. Generally, the immense interfacial area created by nanofillers can influence the behavior of the surrounding polymer matrix even at extraordinarily low content[43], producing a co-continuous network of greatly altered polymer chains[44]. On the other hand, however, the larger interface, the more difficulty in obtaining proper dispersion, thus exacerbates the impregnation. Therefore, the dispersion state of all three types of nanofillers is crucial to determine the final performance of the 2D nanofiller/polymer composites, and it is necessary to understand the effect of the dispersion on the properties of the composites. Herein, we compare the results of the mechanical testing and discuss factors that affected PTT-PTMO based nanocomposites by inorganic (MMT) and organic (GNP, GO) nanoplatelets. The tensile properties of PTT-PTMO based nanocomposites containing 0.5 wt.% of MMT, GNP and GO are presented in Table 3 and representative stress-strain curves are shown in Figure 3. The tensile modulus values slightly increases from 118 to 124 and 133 MPa with an addition of both types of graphene derivatives forms, GO and GNP respectively. On the other hand, however, the presence of organoclay lead to an increase of about 15% (138 MPa) when compared to neat PTT-PTMO. Moreover, an increase in yield stress (σ_y) with an addition of MMT, GNP and GO has been observed. Notwithstanding, the strongest influence on σ_y was observed in the case of PTT-PTMO/0.5GNP, what indicates on good "anchoring" of nanoplatelets in the matrix, which probably is caused by defects, impurities, free radicals, residual functional groups etc. on the surface of GNP that caused grater connection to the copolymer matrix[45]. However, yield elongation did not change significantly for PTT-PTMO/0.5MMT and increased for about 35% for both types of nanocomposites with graphene derivatives form (GNP and GO) when compared to the neat PTT-PTMO copolymer. The tensile strength increase when MMT and GO were added. However, an addition of GNP slightly lowers the value of tensile strength. However, their values are still comparable to neat PTT-PTMO copolymer. For all nanocomposites with an addition of 0.5 wt.% of 2D-type nanofiller, the values of elongation at break are comparable or higher or than the neat PTT-PTMO copolymer. The greatest improvement (the highest value of ε_b) has been observed in the case of PTT-PTMO/0.5GO. As mentioned above, all three types of nanocomposites have comparable values of degree of crystallinity with neat PTT-PTMO copolymer (only slight decrease in the case of PTT-PTMO/0.5GNP). This can indicate that an increase of tensile modulus and yield stress is attributed to the presence of 2D-type nanofillers and the good interfacial bonding between the plateletes' surface and the matrix.

The influence of the MMT, GNP and GO content on the rubber elastic properties of PTT-PTMO block copolymer was determined also during cyclic tensile tests (Fig. 4). The PTT-PTMO based nanocomposites as well as the neat copolymer matrix exhibit a general characteristic, which

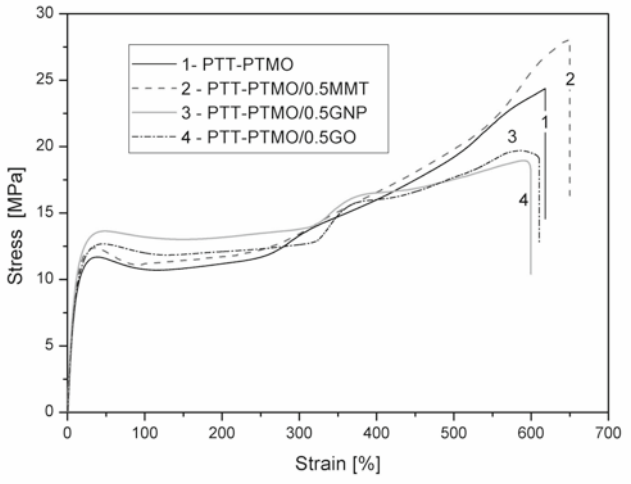

Figure 3. Representative stress-strain curves for nanocomposites and neat PTT-PTMO copolymer

Table 3. Tensile properties of PTT-PTMO based nanocomposites with 0.5 wt.% of MMT, GNP and GO

Sample	*E*	σ_y	ε_y	σ_b	ε_b	PS(100)	PS(200)
	MPa	MPa	%	MPa	%	%	%
PTT-PTMO	118.4 ±2.5	11.9 ±0.1	34.4 ±1.4	24.2 ±1.7	630 ±21	32 ±1	90 ±3
PTT-PTMO/0.5MMT	138.5 ±8.3	12.4 ±0.5	35.7 ±0.6	27.2 ±2.9	643 ±28	34 ±2	94 ±3
PTT-PTMO/0.5GNP	133.0 ±1.7	13.7 ±0.1	48.4 ±0.2	18.2 ±0.3	625 ±23	36 ±3	95 ±3
PTT-PTMO/0.5GO	124.3 ±5.2	12.6 ±0.2	46.1 ±1.1	25.5 ±0.7	647 ±31	35 ±2	94 ±6

E – tensile modulus, σ_y, ε_y – yield stress and strain respectively; σ_b, ε_b – stress and strain at break respectively; PS(100), PS(200) – permanent set was taken as the strain at which zero load was measured on the first unloading cycle to 100 and 200% strain, respectively.

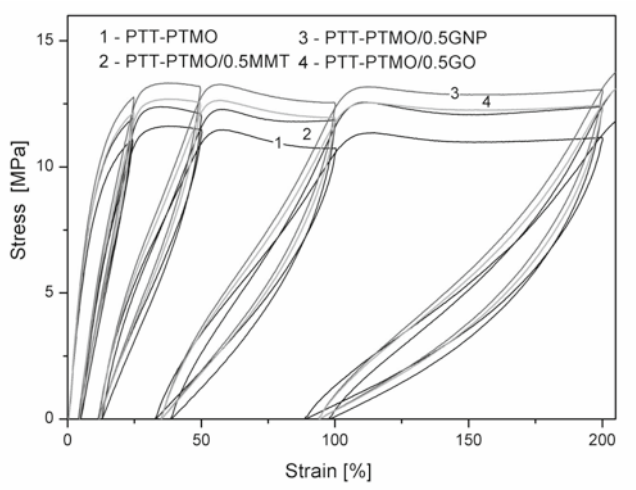

Figure 4. The stress versus strain in cyclic tensile tests with various maximum strains (ε_{max} = 20, 50, 100 and 200%). A representative example of the step-cycle test

are common for thermoplastic block copolymers[34]. This behaviour incorporates a considerable permanent set and a variation in the stress-strain relation every time when a new maximum strain limit is attained by a specimen. Permanent set has been measured as an irreversible strain of the initial specimen's length. The values of permanent set (PS) in the tension's direction, resultant from the maximum attained strain i.e. ε_{max} = 100% and 200% for all three types of nanocomposites containing 2D-type nanofillers and neat PTT-PTMO copolymer are presented in Table 3. For all three types of nanofillers the values of permanent set (PS(100), PS(200)) are slightly higher than for the neat copolymer. Moreover, in each case, the addition of 2D-type nanofillers caused an increase of PS(200) values when compared to the neat copolymer. Since, calorimetric studies obtained for PTT-PTMO/MMT and PTT-PTMO/GO nanocomposites (Table 2) showed small differences in the polymer melt enthalpy (only 1.7 J/g increase for PTT-PTMO/0.5 wt.% MMT, 0.4 J/g decrease for PTT-PTMO/0.5GNP and 1.2 J/g increase for PTT-PTMO/0.5 wt.% GO) and negligible increase in degree of crystallinity, the observed improvement in the tensile properties cannot be due to a change in crystallinity but is more likely caused by the presence of clay or GNP/GO sheets next to PTT hard domains dispersed in PTMO-rich soft phase. The presence of organoclay Nanofil 32, GNP and GO in PTT-PTMO matrix caused an increase in permanent set at 100% strain. It might be due to strong interfacial interaction between nanoplatelets and PTT-PTMO chains. Generally, strong nanofiller-polymer matrix interactions lead to less sliding deformation, thus more stress is needed to break the chain. Nevertheless, the values of permanent set at the strain of 200% are slightly higher than that obtained for the neat copolymer.

CONCLUSIONS

PTT-PTMO block copolymer based nanocomposites containing 0.5 wt.% of inorganic (modified organoclay (Nanofil 32) and organic (graphene nanoplatelets (GNP) and graphene oxide (GO) nanoplatelets were prepared by *in situ* polymerization. As confirmed by transmission electron microscopy (TEM), nanocomposites with randomly distributed 2D-type nanoplatelets throughout whole volume of polymer matrix were obtained. DSC results showed that the glass transition temperature of PTMO-rich soft phase was not affected in the case of an addition of MMT, however, a five degree shift toward lower temperature was seen for PTT-PTMO/GNP and PTT-PTMO/GO. Moreover, the melting temperature of PTT hard phase and degree of crystallinity of the nanocomposites were not influenced by the presence of organoclay and graphene oxide in PTT-PTMO matrix. Moreover, the presence of MMT, GNP and GO in the polymer, affected the shift's effects associated with crystallization. It was assumed about the antinucleating nature of oxidized graphene nanoplatelets as well as about the distinctive nucleating nature of MMT and GNP. Organic (GNP, GO) and inorganic (MMT) nanofillers acted as reinforcing filler in PTT-PTMO matrix, increasing the tensile modulus and yield stress of nanocomposites without decreasing elasticity. The permanent set values for all nanocomposites were comparable to the neat PTT-PTMO copolymer.

ACKNOWLEDGEMENT

Sandra Paszkiewicz and Iwona Pawelec would like to thank for financial support from West Pomeranian University of Technology, Szczecin, (Dean's grant for young scientists). Authors would like to thank DuPont Tate & Lyle BioProducts company for providing bio-1,3-propanediol for experimental use.

LITERATURE CITED

1. Kojima, Y., Usuki, A., Kawasumi, M., Okada, A., Kurauchi, T. & Kamigaito, O. (1993). One-pot synthesis of nylon 6–clay hybrid. *J. Polym. Sci. Pol. Chem.* 31(7), 1755–1758. DOI: 10.1002/pola.1993.080310714.

2. Kawasumi, M. (2004). The discovery of polymer-clay hybrids. *J. Polym. Sci. Pol. Chem.* 42(7), 820–824. DOI: 10.1002/pola.10961.

3. De Paiva, L.B., Morales, A.R. & Valenzuela Díaz, F.R. (2008). Organoclays: Properties, preparation and applications. *Appl. Clay. Sci.* 42(1–2), 8–24. DOI: 10.1016/j.clay.2008.02.006.

4. Lee, A. & Lichtenhan, J.D. (1999). Thermal and viscoelastic property of epoxy–clay and hybrid inorganic–organic epoxy nanocomposites. *J. Polym. Sci. Polym. Chem. Ed.* 37(10), 1993––2001. DOI: 10.1002/(SICI)1097-4628(19990906)73:10<1993::AID-APP18>3.0.CO;2-Q.

5. Suh, D.J., Lim, Y.T. & Park, O.O. (2000). The property and formation mechanism of unsaturated polyester–layered silicate nanocomposite depending on the fabrication methods. *Polymer* 41, 8557–8563. DOI: 10.1016/S0032-3861(00)00216-0.

6. Agag, T., Koga, T. & Takeichi, T. (2001). Studies on thermal and mechanical properties of polyimide±clay nanocomposites. *Polymer* 42, 3399–3408. DOI: 10.1016/S0032-3861(00)00824-7.

7. Chen, G., Liu, S., Chen, S. & Qi, Z. (2001). FTIR spectra, thermal properties, and dispersibility of a polystyrene/montmorillonite nanocomposite. *Macromol. Chem. Phys.* 202(7), 1189–1193. DOI: 10.1002/1521-3935(20010401)202:7<1189::AID-MACP1189>3.0.CO;2-M.

8. Lee, J.W., Lim, Y.T. & Park, O.O. (2000). Thermal characteristics of organoclay and their effects upon the formation of polypropylene/organoclay nanocomposites. *Polym. Bull.* 45(2), 191–198. DOI: 10.1007/s002890070048.

9. Ou, C.F., Ho, M.T. & Lin, J.R. (2004). Synthesis and characterization of poly(ethylene terephthalate) nanocomposites with rganoclay. *J. Appl. Polymer Sci.* 91(1), 140–145. DOI: 10.1002/app.13158.

10. Kim, H., Abdala, A.A. & Macosko, C.W. (2010). Graphene/polymer nanocomposites. *Macromolecules* 43(16), 6515–6530. DOI: 10.1021/ma100572e.

11. Slonczewski, J.C. & Weiss, P.R. (1958). Band structure of graphite. *Phys. Rev.* 109(2), 272. DOI: 10.1103/PhysRev.109.272.

12. Bunch, J.S., Verbridge, S.S., Alden, J.S., Van der Zande, A.M., Parpia, J.M., Craighead, H.G. & McEuen, P.L. (2008). Impermeable atomic membranes from graphene sheets. *NanoLett*. 8(8), 2458–2462. DOI: 10.1021/nl801457b.

13. Du, X., Skachko, I., Barker, A. & Andrei, E.Y. (2008). Approaching ballistic transport in suspended graphene. *Nature Nanotechnol.* 3(8), 491–495. DOI: 10.1038/nnano.2008.199.

14. Balandin, A.A., Ghosh, S., Bao, W., Calizo, I., Teweldebrhan, D., Miao, F. & Lau, C.N. (2008). Superior thermal conductivity of single-layer graphene. *NanoLett.* 8(3), 902–907. DOI: 10.1021/nl0731872.

15. Lee, C., Wei, X., Kysar, J.W. & Hone, J. (2008). Measurement of the elastic properties and intrinsic strength of monolayer graphene. *Science* 321(5887), 385–388. DOI: 10.1126/science.1157996.

16. Jinhong, Y., Huang, X., Wu, C. & Jiang, P. (2011). Permittivity, thermal conductivity and thermal stability of poly(vinylidene fluoride)/graphene nanocomposites. *IEEE T. Dielect. El. In.* 18(2), 478–484. DOI: 10.1109/TDEI.2011.5739452.

17. Chen, Y., Qi, Y., Tai, Z., Yan, X., Zhu, F. & Xue, Q. (2012). Preparation, mechanical properties and biocompatibility of graphene oxide/ultrahigh molecular weight polyethylene composites. *Europ. Polym. J.* 48(6), 1026–1033. DOI: 10.1016/j.eurpolymj.2012.03.011.

18. Beckert, F., Friedrich, C., Thomann, R. & Mülhaupt, R. (2012). Sulfur-functionalized graphenes as macro-chain-transfer and RAFT agents for producing graphene polymer Brushes and polystyrene nanocomposites. *Macromolecules* 45(17), 7783–7090. DOI: 10.1021/ma301379z.

19. Potts, J.R., Lee, S.H., Alam, T.M., An, J., Stoller, M.D., Piner, R.D. & Ruoff, R.S. (2011). Thermomechanical properties of chemically modified graphene/poly (methyl methacrylate) composites made by in situ polymerization. *Carbon* 49(8), 2615–2623. DOI: 10.1016/j.carbon.2011.02.023.

20. Zhang, F., Peng, X., Yan, W., Peng, Z. & Shen, Y. (2011). Non- isothermal crystallization kinetics of in situ Nylon 6/graphene composites by differential scanning calorimetry. *J. Polym. Sci. Phys.* 49(19), 1381–1388. DOI: 10.1002/polb.22321.

21. Wang, X., Hu, J., Song, L., Yang, H., Xing, W. & Lu, H. (2011). *In situ* polymerization of graphene nanosheets and polyurethane with enhanced mechanical and thermal properties. *J. Mater. Chem.* 21(12), 4222–4227. DOI: 10.1039/C0JM03710A.

22. Fabbri, P., Bassoli, E., Bon, S.B. & Valentini, L. (2012). Preparation and characterization of poly (butylene terephthalate)/graphene composites by *in situ* polymerization of cyclic butylene terephthalate. *Polymer* 53(4), 897–902. DOI: 10.1016/j.polymer.2012.01.015.

23. Istrate, O.M., Paton, K.R., Khan, U., O'Neill, A., Bell, A.P. & Coleman, J.N. (2014). Reinforcement in melt-processed polymer–graphene composites at extremely low graphene loading level. *Carbon* 78, 243–249. DOI: 10.1016/j.carbon.2014.06.077.

24. Paszkiewicz, S. Roslaniec, Z., Szymczyk, A., Spitalsky, Z. & Mosnacek, J. (2012). Morphology and thermal properties of expanded graphite (EG)/poly(ethylene terephthalate) (PET) nanocomposites. *Chemik* 66(1), 26–30.

25. Paszkiewicz, S. Nachman, M., Szymczyk, A., Spitalsky, Z., Mosnacek, J. & Roslaniec, Z. (2014). Influence of expanded graphite (EG) and graphene oxide (GO) on physical properties of PET based nanocomposites. *Pol. J. Chem. Technol.* 16(4), 45–50. DOI: 10.2478/pjct-2014-0068.

26. Tantis, I., Psarras, G.C. & Tasis, D. (2012). Functionalized graphene – poly(vinyl alcohol) nanocomposites: Physical and dielectric properties. *eXPRESS Polym. Lett.* 6(4), 283–292. DOI: 10.3144/expresspolymlett.2012.31.

27. Steurer, P., Wissert, R., Thomann, R. & Muelhaupt, R. (2009). Functionalized graphenes and thermoplastic nanocomposites based upon expanded graphite oxide. *Macromol. Rapid Commun.* 30(4–5), 316–327. DOI: 10.1002/marc.200800754.

28. Van der Schuur, M. & Gaymans, R. (2007). Influence of morphology on the properties of segmented block copolymers. *Polymer* 48(7), 1998–2006. DOI: 10.1016/j.polymer.2007.01.063.

29. Paszkiewicz, S. Szymczyk, A., Špitalski, Z., Mosnáček, J., Kwiatkowski, K. & Rosłaniec, Z. (2014). Structure and properties of nanocomposites based on PTT-block-PTMO copolymer and graphene oxide prepared by *in situ* polymerization. *Europ. Polym. J.* 50, 69–77. DOI: 10.1016/j.eurpolymj.2013.10.031.

30. Szymczyk, A. Paszkiewicz, S. & Roslaniec, Z. (2013). Influence of intercalated organoclay on the phase structure and physical properties of PTT–PTMO block copolymers. *Polym. Bull.* 70(5), 1575–1590. DOI: 10.1007/s00289-012-0859-y.

31. Spitalsky, Z., Danko, M. & Mosnacek, J. (2011). Preparation of functionalized graphene sheets. *Current Oragan. Chem.* 15(8), 1133–1150. DOI: 10.2174/138527211795202988.

32. Paszkiewicz, S., Szymczyk, A., Livanov, K., Wagner, H.D. & Roslaniec, Z. (2015). Enhanced thermal and mechanical properties of poly(trimethylene terephthalate-block-poly(tetramethylene oxide) segmented copolymer based hybrid nanocomposites prepared by *in situ* polymerization via synergy effect between SWCNTs and graphene nanoplatelets. *eXPRESS Polym. Lett.* 9(6), 509–524. DOI: 10.3144/expresspolymlett.2015.49.

33. Pilawka, R., Paszkiewicz, S. & Rosłaniec, Z. (2014). Thermal degradation kinetics of PET/SWCNTs nanocomposites prepared by the *in situ* polymerization. *J. Therm. Anal. Calorim.* 115(1), 451–460. DOI: 10.1007/s10973-013-3239-4.

34. Szymczyk, A., Nastalczyk, J., Sablong, R.J. & Roslaniec, Z. (2011). The influence soft segment length on structure and properties of poly(trimetylene terephthalate)-block-poly(tetramethylene oxide) segmented random copolymers. *Polym. Adv. Technol.* 21(1), 72–83. DOI: 10.1002/pat.1858.

35. Pyda, M., Boller, A., Grebowicz, J., Chuah, H., Lebedev, B. V. & Wunderlich, B. (1998). Heat capacity of poly(trimethylene terephthalate). *J. Polym. Sci. Phys.* 36(14), 2499–2511. DOI: 10.1002/(SICI)1099-0488(199810)36:14<2499::AID-POLB4>3.0.CO;2-O.

36. Kim, H., Miura, Y. & Macosko, C.W. (2010). Graphene/Polyurethane Nanocomposites for Improved Gas Barrier and Electrical Conductivity. *Chem. Mater*. 22, 3144–3450. DOI: 10.1021/cm100477v.

37. Hernández, M., del Mar Bernal, M., Verdejo, R. & Ezquerra, T.A. (2012). Overall performance of natural rubber/graphene nanocomposites. *Compos. Sci. Technol*. 73, 40–46. http://dx.doi.org/10.1016/j.compscitech.2012.08.012

38. Lewis, S.L. (2007). *Interface Control in Polymer Nanocomposites*. Doctoral dissertation, Rensselaer Polytechnic Institute, Troy, New York, USA.

39. Martin-Gallego, M., Verdejo, R., Lopez-Manchado, M.A. & Sangermano, M. (2011). Epoxy–graphene UV-cured nanocomposites. *Polymer* 52(21), 4664–4669. DOI: 10.1016/j.polymer.2011.08.039.

40. Lee, J.K., Song, S. & Kim, B. (2012). Functionalized graphene sheets-epoxy based nanocomposites for cryotank composite applications. *Polym. Compos.* 33(8), 1263–1273. DOI: 10.1002/pc.22251.

41. Torre, L., Lelli, G. & Kenny, J.M. (2006). Synthesis and characterization of sPS/montmorillonite nanocomposites. *J. Appl. Polym. Sci.* 100(6), 4957–4963. DOI: 10.1002/app.23803.

42. Ilčíková, M., Mosnáček, J., Mrlík, M., Sedláček, T., Csomorová, K., Czaniková, K. & Krupa, I. (2014). Influence of surface modification of carbon nanotubes on interactions with polystyrene-*b*-polyisoprene-*b*-polystyrene matrix and its photo--actuation properties. *Polym. Adv. Technol.* 25 (11), 1293–1300. DOI: 10.1002/pat.3324.

43. Desai, T., Keblinski, P. & Kumar, S.K. (2005). Molecular dynamics simulations of polymer transport in nanocomposites. *J. Chem. Phys.* 122(13), 134910–134918. DOI: 10.1063/1.1874852.

44. Bansal, A., Yang, H., Li, C., Cho, K., Benicewicz, B.C., Kumar, S.K. & Schadler, L.S. (2005). Quantitative equivalence between polymer nanocomposites and thin polymer films. *Nat. Mater.* 4(9), 693–698. DOI: 10.1038/nmat1447.

45. Paszkiewicz, S. (2014). *Polymer hybrid nanocomposites containing carbon nanoparticles. In situ synthesis and physical properties*. Doctoral dissertation, West Pomeranian University of Technology, Szczecin, Poland.